

1 **Exploring the relationship between warm-season precipitation, potential evaporation, and**
2 **“apparent” potential evaporation at site scale**

3 Xi Chen¹ and Steven G. Buchberger²

4 ¹College of Arts and Sciences, Department of Geography and Geographic Information Science,
5 University of Cincinnati

6 ²College of Engineering and Applied Science, Department of Civil Engineering and
7 Architectural Engineering and Construction Management, University of Cincinnati

8 Corresponding author: Xi Chen (xi.chen@uc.edu)

9

10

11

12

13

14

15

16

17

18

19

20

21 **Abstract**

22 Bouchet’s complementary relationship and the Budyko hypothesis are two classic frameworks
23 that are inter-connected. To systematically investigate the connections between the two
24 frameworks, we analyze precipitation, pan evaporation and potential evaporation data at 259
25 weather stations across the United States. The precipitation and pan evaporation data are from
26 field measurement and the potential evaporation data are collected from a remote-sensing
27 dataset. We use pan evaporation to represent “apparent” potential evaporation, which is different
28 from potential evaporation. With these data, we study the correlations between precipitation and
29 potential evaporation, and between precipitation and “apparent” potential evaporation. The
30 results show that 93% of the study weather stations exhibit a negative correlation between
31 precipitation and “apparent” potential evaporation. Also, the aggregated data cloud of
32 precipitation versus “apparent” potential evaporation with 5312 warm-season data points from
33 259 weather stations shows a negative trend in which “apparent” potential evaporation decreases
34 with increasing precipitation. On the other hand, no significant correlation is found in the data
35 cloud of precipitation versus potential evaporation, indicating that precipitation and potential
36 evaporation are independent. We combine a Budyko-type expression, the Turc-Pike equation,
37 with Bouchet’s complementary relationship to derive upper and lower Bouchet-Budyko curves,
38 which display a complementary relationship between “apparent” potential evaporation and actual
39 evaporation. The observed warm-season data follow the trend of the Bouchet-Budyko curves.
40 Our study shows the consistency between Budyko’s framework and Bouchet’s complementary
41 relationship, with the distinction between potential evaporation and “apparent” potential
42 evaporation. The formulated complementary relationship can be used in quantitative modeling
43 practices.

44 **1. Introduction**

45 Potential evaporation (E_p) is a widely used physical variable in hydrologic frameworks. It is the
46 evaporation rate under unlimited land surface water supply (Thornthwaite, 1948). Pan
47 evaporation (E_{pan}) measurement is often used as a surrogate of potential evaporation. However,
48 these two variables are not the same (Brutsaert and Parlange, 1998; Roderick et al., 2009). A
49 stipulation is added in the potential evaporation definition in Van Bavel (1966) and further
50 clarified in Brutsaert (2015) that: “the surface vapor pressure be saturated, so that it can be found
51 from the surface temperature.” Therefore, the main difference between potential evaporation and
52 pan evaporation is that pan evaporation is not measured under saturated surface vapor pressure.
53 As a result, potential evaporation can be considered to depend only on the energy supply of
54 climate while pan evaporation is driven by both energy supply and humidity deficit in the
55 atmosphere (Rotstayn et al., 2006). In Brutsaert and Parlange (1998), the term “apparent”
56 potential evaporation (E_{pa}) is introduced to distinguish pan evaporation from potential
57 evaporation. “Apparent” potential evaporation can be measured by an evaporation pan, while
58 potential evaporation cannot. We acknowledge that there are different definitions of potential
59 evaporation in the literature (Aminzadeh et al., 2016). Our study follows the definition of
60 potential evaporation in Brutsaert and Parlange (1998) and Brutsaert (2015).

61 Because potential evaporation is energy-driven, it can be used as a physical variable to
62 describe the energy supply in a hydrologic system. For instance, the well-established Budyko
63 framework (Budyko, 1958; 1974) uses precipitation (P) and potential evaporation to represent
64 the relationship between water supply and energy supply, and therefore to describe the impact of
65 long-term climate on the hydrologic cycle. The Budyko framework has been extensively used to
66 analyze interactions between hydrology, climate, vegetation and other elements in watersheds

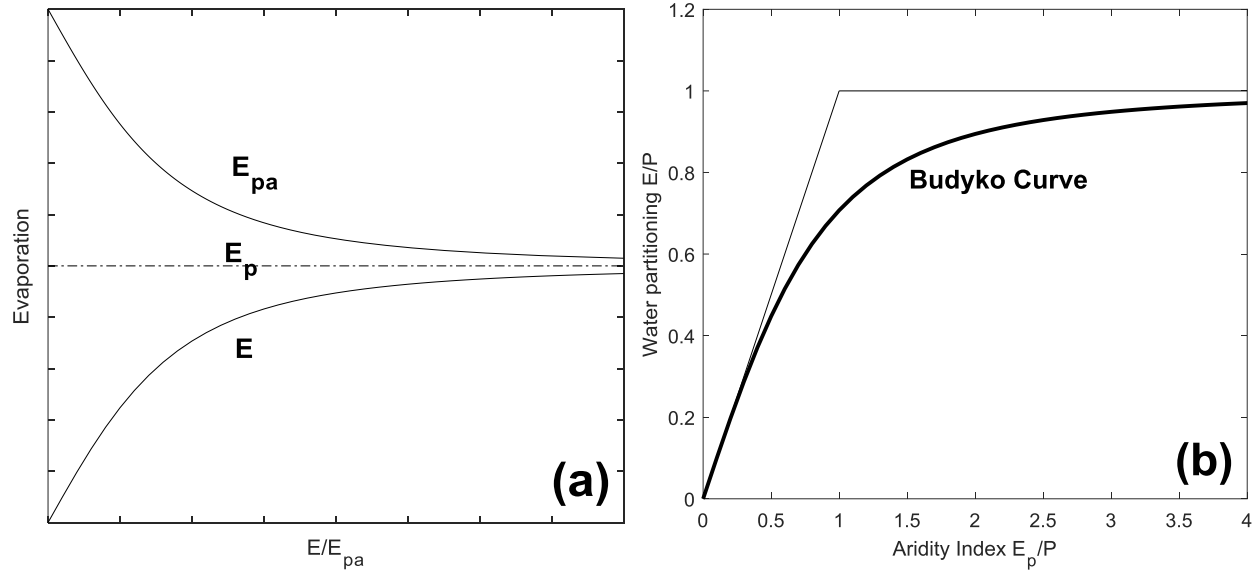
67 (Milly, 1994; Zhang et al., 2001; Yang et al., 2007; Donohue et al., 2007; Yang et al., 2011; Xu
68 et al., 2014; Zhou et al., 2015; Zhou et al., 2016). Furthermore, the Budyko framework, which is
69 originally applicable at the long-term mean annual scale, has been extended to shorter time
70 scales, such as annual (Wang and Alimohammadi, 2012; Zhang et al., 2008) and intra-annual
71 periods (Chen et al., 2013).

72 Several studies have made connections between the Budyko framework and Bouchet's
73 complementary relationship (CR) (Bouchet, 1963). Yang et al. (2006) used the Fu equation (Fu,
74 1981), which is one of the commonly used equations to represent the Budyko curve, to describe
75 the relationship between actual evaporation and potential evaporation in the CR. Roderick et al.
76 (2009) presented a complementary relationship normalized by net irradiance and compared it
77 with the Budyko framework. Lhomme and Moussa (2016) combined Turc-Pike equation (Turc,
78 1954; Pike, 1964), which is another commonly used Budyko-type equation, with the CR to show
79 the dependence of Budyko curve on the drying power of the air.

80 When linking the Budyko framework with the CR, it is crucial to have a clear definition
81 of different types of evaporation used in these two frameworks. Brutsaert and Parlange (1998)
82 and Brutsaert (2015) generalized the CR and provided definitions of the evaporation terms in the
83 CR, namely actual evaporation (E), potential evaporation (E_p), and "apparent" potential
84 evaporation (E_{pa} , see Fig. 1a). Brutsaert and Parlange (1998) point out that the complementary
85 relationship is between actual evaporation and "apparent" potential evaporation, not between
86 actual evaporation and potential evaporation. In the Budyko framework (Fig. 1b), the definition
87 of potential evaporation follows Van Bavel (1966)'s potential evaporation definition that it is
88 under unlimited land surface water supply without the effect of humidity deficit (Budyko, 1974),
89 which is the same as the E_p definition in the generalized CR. The definitions of evaporation,

90 potential evaporation and “apparent” potential evaporation in these different frameworks are
91 summarized in Table 1.

92 Process-based speaking, the CR suggests a connection between evaporation and
93 “apparent” potential evaporation (Fig. 1a), which is driven by the energy feedbacks between
94 atmosphere and land surface. During the drying process at the land surface, the excessive energy
95 that is not used for evaporation will be available for the increase of sensible heat. The rise in air
96 temperature will lead to an increase in the rate of “apparent” potential evaporation (Brutsaert and
97 Parlange, 1998; Brutsaert, 2005; Aminzadeh et al., 2016). This connection between E_{pa} and E
98 also suggests a connection between E_{pa} and P , since the water supply from precipitation will
99 affect the rate of evaporation. In terms of the Budyko framework, E_p and P are used as the
100 representations of energy supply and water supply respectively. The ratio between E_p and P is
101 the primary controlling factor of the ratio of E over P in watersheds at long-term mean annual
102 time scale (Fig. 1b). The ratio of E_p over P is also called the aridity index, which represents the
103 dryness of the climate in a watershed. The ratio of E over P increases with the increase of aridity
104 index, indicating that more water from precipitation will become evaporation rather than runoff
105 under drier climate (Arora, 2002). No connection between E_p and P is suggested in the Budyko
106 framework.



107
 108 Fig. 1. Conceptual representations of (a) the complementary relationship and (b) Budyko
 109 framework.

110 Table 1. Types of evaporation in the Budyko framework and the original CR, and their redefined
 111 evaporation type based on generalized CR. The last column refers to the definitions of the three
 112 types of evaporation in the generalized CR provided in Brutsaert (2015).

Budyko Framework	Bouchet's Complementary Relationship	Generalized Complementary Relationship	Evaporation Definitions in Brutsaert (2015)
Actual evaporation (E)	Actual evaporation (E)	Actual evaporation (E)	The first type
Potential evaporation (E_p)	Wet environment evaporation (E_0)	Potential evaporation (E_p)	The second type
-	Potential evaporation (E_p)	“Apparent” potential evaporation (E_{pa})	The third type

113
 114 In order to explore the connections between the Budyko framework and the CR, our
 115 study investigates the relationships between precipitation and potential evaporation as well as
 116 between precipitation and “apparent” potential evaporation. We collect warm-season
 117 precipitation, potential evaporation and pan evaporation data from 259 weather stations across
 118 the contiguous US. Studying the relationships between P , E_p and E_{pa} , advances our

119 understanding of the well-established classic Budyko framework and the CR. Furthermore,
120 based on insights provided by previous studies (Yang et al., 2006; Roderick et al., 2009;
121 Lhomme and Moussa, 2016), we use a Budyko-type expression to develop a new formulation for
122 the CR.

123

124 **2. Methodology**

125 2.1 Theoretical development

126 2.1.1 Budyko framework

127 The Budyko curve (Fig. 1b) describes the relationship between long-term water partitioning,
128 represented by the ratio of actual evaporation over precipitation, and long-term climate,
129 represented by the ratio of potential evaporation over precipitation, namely aridity index
130 (Budyko, 1958; 1974). In recent decades, the Budyko framework has been examined with
131 annual data (e.g. Yang et al., 2007; Potter and Zhang, 2009; Cheng et al., 2011). A number of
132 Budyko-type functions have been developed to mathematically describe the Budyko curve (Turc,
133 1954; Fu, 1981; Zhang et al., 2001; Yang et al., 2008; Wang and Tang, 2014). Within these
134 functions, the Turc-Pike equation is a parsimonious single parameter equation (Turc, 1954; Pike,
135 1964):

$$136 \quad \frac{E}{P} = \left[1 + \left(\frac{E_p}{P} \right)^{-\nu} \right]^{-\frac{1}{\nu}} \quad (1)$$

137 where E is actual evaporation, E_p is potential evaporation, P is precipitation, and ν is a parameter
138 to represent landscape properties such as vegetation coverage and soil properties (Zhang et al.,

139 2001; Yang et al., 2008). The parameter ν needs to be a positive number, and its typical value is
140 2.0.

141 2.1.2 Generalized complementary relationship

142 Bouchet's complementary relationship (Bouchet, 1963) describes the relationship between actual
143 evaporation E and potential evaporation E_p . Brutsaert and Parlange (1998) introduced the term
144 "apparent" potential evaporation E_{pa} and clarified that the CR is between E and E_{pa} , not E and E_p
145 (Fig. 1a). They also proposed a generalized complementary relationship:

$$146 \quad bE + E_{pa} = (1 + b)E_p \quad 0 \leq E \leq E_p \leq E_{pa} \quad (2)$$

147 where b is a proportionality parameter not less than one. When b is equal to one, Eq. (2)
148 represents the original complementary relationship (Kahler and Brutsaert, 2006). "Apparent"
149 potential evaporation will be higher than potential evaporation, especially under dry conditions;
150 while it gradually approaches potential evaporation as the ratio of E over E_{pa} increases (Fig. 1a).
151 As suggested by Morton (1976) and Brutsaert and Stricker (1979), potential evaporation can be
152 estimated using the Priestley-Taylor equation (Priestley and Taylor, 1972), which is also called
153 equilibrium evaporation (Brutsaert and Chen, 1995; Jiang and Islam, 2001). "Apparent"
154 potential evaporation can be estimated using the Penman equation (Penman, 1948; Linacre,
155 1994; Rotstayn et al., 2006) or using data measured at evaporation pans (Brutsaert, 1982;
156 Brutsaert and Parlange, 1998):

$$157 \quad E_{pa} = aE_{pan} \quad (3)$$

158 where E_{pan} is the pan evaporation and a is the pan coefficient. The pan coefficient varies from
159 location to location (Stanhill, 1976; Linacre, 1994). In Kahler and Brutsaert (2006), a pan

160 coefficient of $a = 1.0$ is recommended for mixed natural vegetation, which will be used in this
 161 study. It should be noted that the linear relationship between E_{pa} and E_{pan} given in Eq. (3) and
 162 the choice of “ a ” value will not affect the correlations between P , E_p and E_{pa} .

163 2.1.3 Relationships between P , E_p and E_{pa}

164 The x-axis of the complementary relationship is a ratio between E and E_{pa} (Bouchet, 1963).
 165 Ramírez et al. (2005) used the water-energy framework to link the CR with Budyko approach
 166 and changed the x-axis in the CR to moisture availability. Following this idea, several studies
 167 have used precipitation or wetness index (P/E_p) to represent moisture availability in the CR
 168 (Yang et al., 2006; Roderick et al., 2009). In this study, we also use P to represent moisture
 169 availability in the CR. E_p is a horizontal line in the CR that is parallel to the x-axis (Fig. 1a).
 170 Therefore, the modified CR indicates that P and E_p are independent. On the other hand, the
 171 upper curve of the CR, representing “apparent” potential evaporation E_{pa} , declines along the x-
 172 axis, indicating that E_{pa} and P are not independent. For a dimensionless CR, we normalize the x
 173 and y axes. The normalized CR describes the relationship between $\frac{E_{pa}}{E_p}$, $\frac{E}{E_p}$, and $\frac{P}{E_p}$ (Fig. 2).

174 To connect the Budyko framework with the normalized CR toward formulating the
 175 Bouchet-Budyko curves, we first transform Eq. (1) into a relationship between $\frac{E}{E_p}$ and $\frac{P}{E_p}$:

$$176 \quad \frac{E}{E_p} = \left[\left(\frac{P}{E_p} \right)^{-v} + 1 \right]^{-\frac{1}{v}} \quad (4)$$

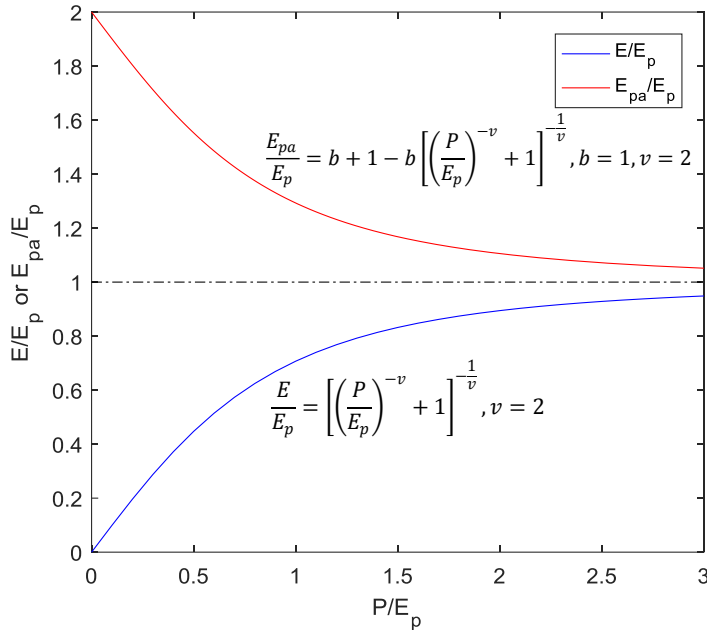
177 Yang et al. (2006) did similar transformation using the Fu equation (Fu, 1981). Dividing both
 178 sides of Eq. (2) by E_p yields:

$$179 \quad b \frac{E}{E_p} + \frac{E_{pa}}{E_p} = 1 + b \quad (5)$$

180 Combining Eqs. (4) and (5), gives a relation between $\frac{P}{E_p}$ and $\frac{E_{pa}}{E_p}$:

181
$$\frac{E_{pa}}{E_p} = b + 1 - b \left[\left(\frac{P}{E_p} \right)^{-v} + 1 \right]^{-1/v} \quad E_{pa} \geq E_p \quad (6)$$

182 Equations (4) and (6) represent the lower and upper curves of the normalized CR
 183 respectively (Fig. 2). Roderick et al. (2009) presented a similar framework, without the
 184 formulation of the curves. To verify the relationships between P , E_p , and E_{pa} , and to examine the
 185 Bouchet-Budyko curves in Eqs. (4) and (6), we analyze climate data from 259 weather stations
 186 across the contiguous US.



188 Fig. 2. Dimensionless Bouchet-Budyko curves in the normalized complementary relationship.

189 2.2 Data sources

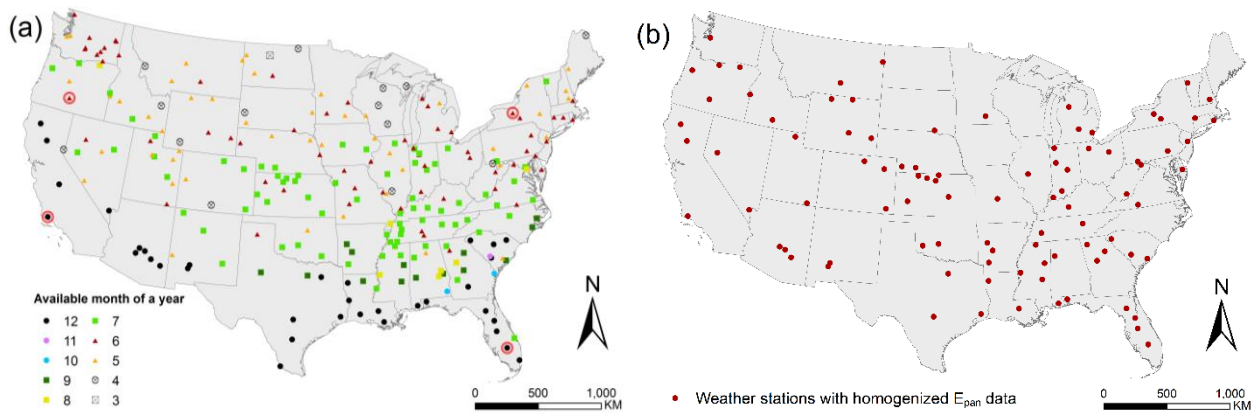
190 Monthly precipitation and pan evaporation are collected from the National Oceanic and
 191 Atmospheric Administration (NOAA) at the National Climatic Data Center (NCDC). The data
 192 can be downloaded at: <https://www.ncdc.noaa.gov/IPS/cd/cd.html> . The precipitation data are

193 measured using standard rain gauge and the pan evaporation data using Class A evaporation
194 pans. We collect data for the period 1984-2015 from a total of 259 weather stations (Fig. 3a).
195 Since pan evaporation is collected only during warm months (when temperatures remain above
196 freezing), the weather stations at cold regions have less than 12 months of pan readings in a year.
197 We call the period of warm months in a year “warm-season”. We calculate the monthly average
198 pan evaporation and precipitation using only the warm months for each year at each weather
199 station. For short, it is called warm-season data (i.e., warm-season pan evaporation, warm-
200 season precipitation). We also calculate the annually averaged warm-season data to represent the
201 long-term average level of pan evaporation and precipitation at each station. For short, it is
202 called long-term average data. Over the 259 selected stations, there is an average of seven
203 months per year with available pan evaporation data. As Fig. 3 shows, the number of available
204 months decreases from the southern regions to the northern regions. For stations in the southern
205 states with all 12 months of available data in a year, the full year will be considered as a warm-
206 season. The northern state stations have fewer warm months, and, accordingly, the warm-season
207 is much shorter. On the other hand, not all 259 weather stations have the full record from 1984
208 to 2015, the average number of years with available data for each location is 18. A complete
209 summary of the information available at all 259 weather station is provided in Table S1. In order
210 to minimize the uncertainty from various warm periods in a year from station to station, we
211 repeat the analysis using an alternative source of pan evaporation in the NCDC dataset
212 containing homogenized warm month data from May to October (Hobbins, et al., 2017). A total
213 of 93 weather stations overlap both sets of pan evaporation data for the period 1984 to 2001 (Fig.
214 3b). We convert pan evaporation in the NCDC dataset to “apparent” potential evaporation using
215 Eq. (3).

216 The E_p data are collected from a remote-sensing dataset (Zhang et al., 2010), which is
 217 generated using the Priestley-Taylor equation with remotely sensed net radiation:

$$218 \quad \lambda E_p = \alpha \frac{\Delta}{\Delta + \gamma} (R_n - G) \quad (7)$$

219 where λ (J/kg) is the latent heat of vaporization; λE_p (W/m^2) is the latent heat flux; α is a
 220 coefficient to account for the effect of surface characteristics and vegetation, and is set to 1.26; Δ
 221 ($\text{Pa}/^\circ\text{C}$) is the slope of the saturated vapor pressure curve; γ ($\text{Pa}/^\circ\text{C}$) is the psychrometric constant;
 222 R_n (W/m^2) is the net radiation; and G (W/m^2) is the heat flux into the ground. The E_p data cover
 223 the period 1983-2006. Similar with P and E_{pa} , we calculate the warm-season E_p and long-term
 224 annually averaged E_p based on the monthly E_p data.



226 Fig. 3. (a) Map of 259 weather stations. The available month of a year of pan evaporation data
 227 for each weather station is presented using legends with different colors and shapes. Four
 228 representative weather stations are selected from the four quadrants of the US respectively,
 229 which are highlighted with red circles. (b) Map of 93 weather stations with homogenized pan
 230 evaporation data that overlap the 259-station dataset.

231 2.3 P , E_p and E_{pa} correlation analysis

232 Using the collected weather station data of precipitation and pan evaporation for the period 1984
233 to 2015, we first calculate the Pearson correlation coefficient between warm-season P and warm-
234 season E_{pa} for each location (Fig. 3a). We then perform the same correlation analysis of P and
235 E_{pa} using the homogenized pan evaporation dataset (Hobbins et al., 2017) (Fig. 3b). Secondly,
236 we use data of warm-season P and warm-season E_p for the period of 1984 to 2006, which is the
237 period both P and E_p data are available, to investigate the correlation between P and E_p . Finally,
238 to validate the newly derived Bouchet-Budyko curves, the relationship between $\frac{P}{E_p}$ and $\frac{E_{pa}}{E_p}$ is
239 plotted using the collected data at both seasonal and long-term average time scales.

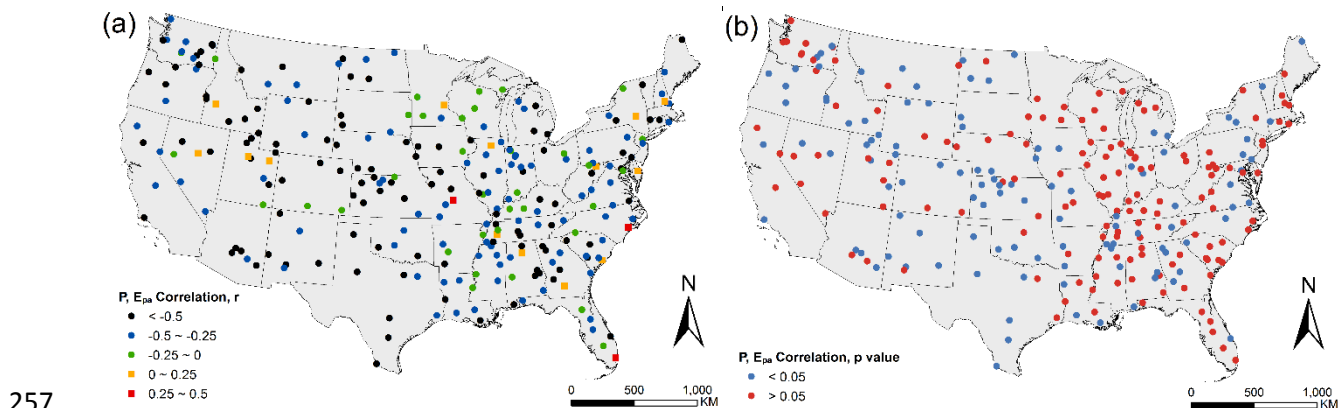
240

241 **3. Results**

242 3.1 Correlations among P , E_p , and E_{pa}

243 In the 259 weather stations, 93% of the stations have a negative correlation between P and E_{pa}
244 (Fig. 4a), but only 43% of the stations are statistically significant ($p < 0.05$; Fig. 4b). All
245 significant P , E_{pa} correlations are negative. The weather stations located in the western region
246 (regions with longitude higher than the weather station average longitude of W 94.81°) are more
247 likely to have a significant P , E_{pa} negative correlation than those located in the east (regions with
248 longitude lower than W 94.81°). This spatial difference may be related to climate characteristics:
249 the eastern region has higher precipitation (averagely 105.5 mm/month) and lower “apparent”
250 potential evaporation (averagely 145.3 mm/month), while the western region has lower
251 precipitation (averagely 44.6 mm/month) and higher “apparent” potential evaporation (averagely
252 203.5 mm/month). The Bouchet’s complementary relationship is more significant in arid regions
253 (Ramírez et al., 2005), corresponding to the left side of the CR curves; while it is less significant

254 in humid regions, corresponding to the right side of the CR curves (Fig. 1a). As a result, the
255 negative correlation between precipitation and “apparent” potential evaporation is more
256 significant in the west than in the east.

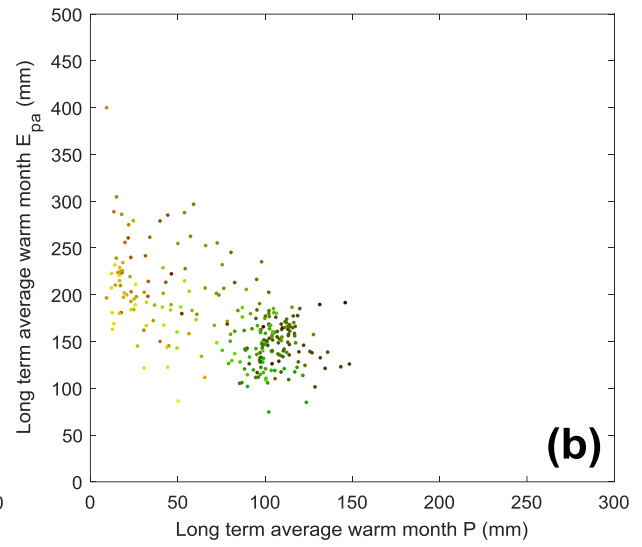
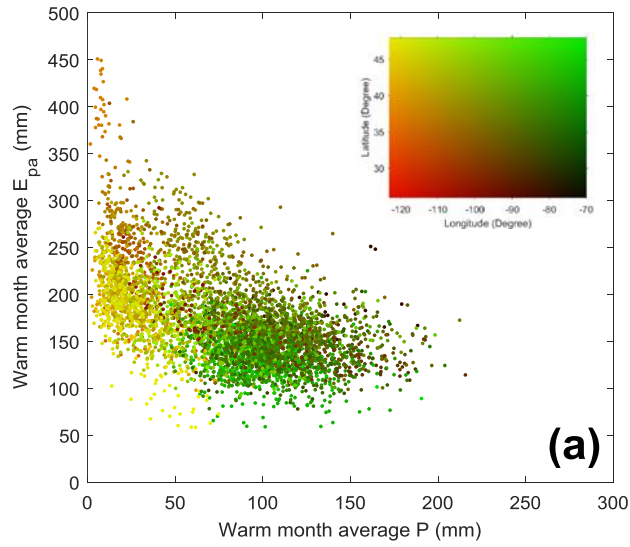


258 Fig. 4. Map of point-scale annual P , E_{pa} correlation at 259 weather stations, (a) r value and (b) p
259 value.

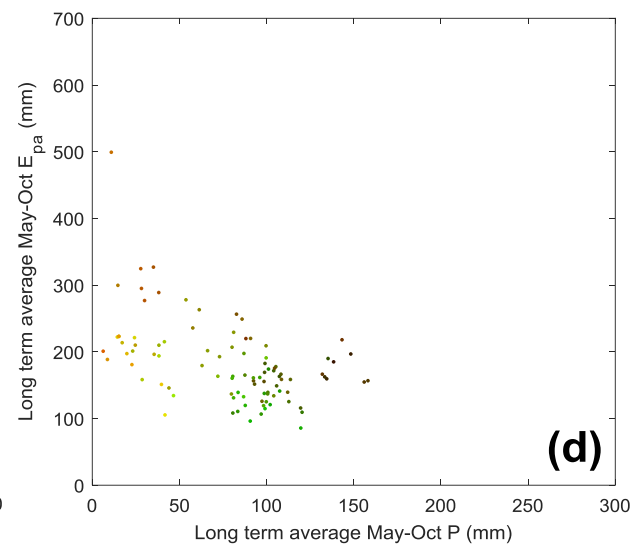
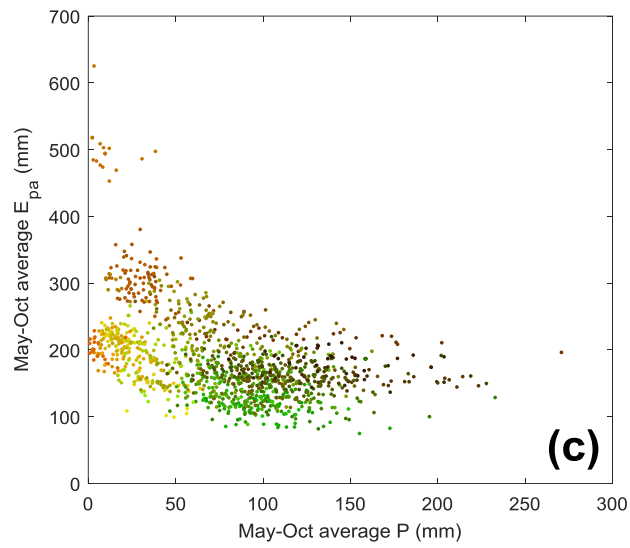
260 All the warm-season P vs. E_{pa} relations (i.e., all years, all seasons, for a total of 5312 data
261 points) are shown in Fig. 5a. The data cloud shows a negative trend in general. We also plot the
262 long-term annually averaged values of warm-season P and E_{pa} of the 259 weather stations (Fig.
263 5b), which shows a similar negative trend. Hobbins et al. (2004) showed a similar negative trend
264 between precipitation and pan evaporation with watershed scale data. To represent the spatial
265 distribution of the weather stations, we color code the data points based on their spatial
266 coordinates of latitude and longitude. The climate in the eastern US is much wetter than the
267 western US, and therefore the data cloud of E_{pa} vs. P is separated into two parts horizontally.
268 The right side of the cloud represents the northeastern and southeastern US (green and brown,
269 respectively); while the left side of the cloud generally represents the northwestern and
270 southwestern US (yellow and red, respectively).

271 As explained before, we also use an alternative pan evaporation dataset (Hobbins et al.,
272 2017) to further validate our analysis result. This dataset is homogenized to have the same
273 period of pan evaporation data record in each year from May to October. In order to minimize
274 the data heterogeneity caused by station move and human errors, this dataset compiled pan
275 evaporation data from 247 stations across the US with thorough quality control. It is derived
276 from the same dataset as our data, namely the NCDC dataset. Based on the homogenized pan
277 evaporation data, 85 stations out of 93 (91%) have a negative correlation between P and E_{pa} . Of
278 these, 41% of the stations have a statistically significant relationship ($p < 0.05$); all negative. This
279 result is consistent with the analysis result based on our collected data from 259 weather stations.
280 We also use the data cloud to show the relationship between P and E_{pa} in the warm period of
281 May to October in each year at each of the 93 stations (Fig. 5c), as well as the relationship of
282 long-term annually averaged warm period P and E_{pa} (Fig. 5d). The trend of data cloud is similar
283 with the data cloud trend using our collected data at both seasonal and long-term average time
284 scales. In other words, both datasets show a negative relationship between P and E_{pa} .

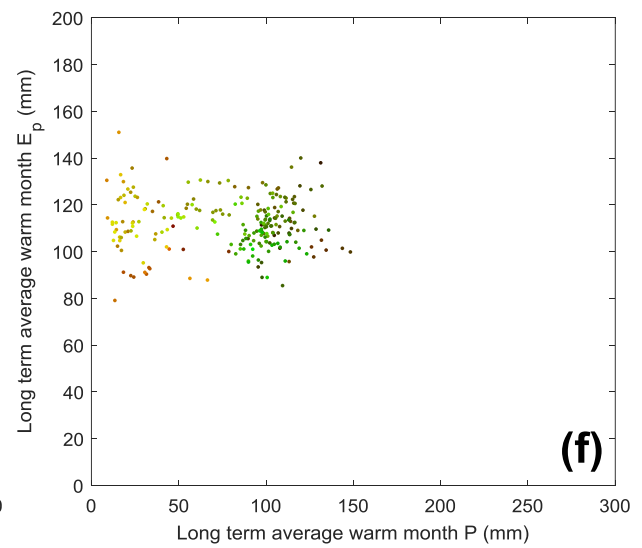
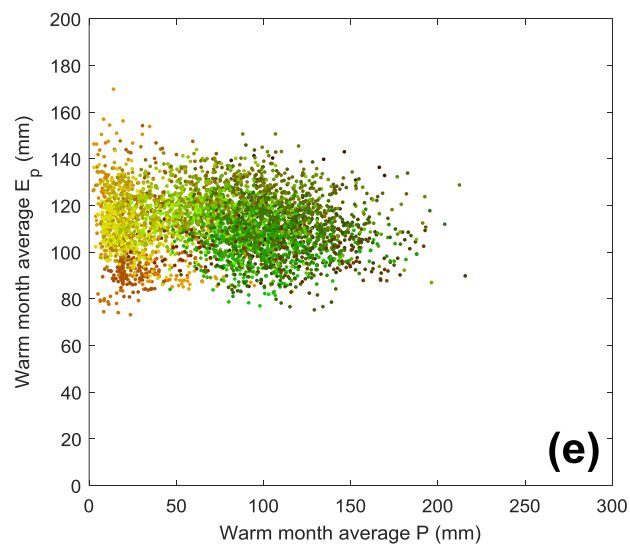
285 The P and E_p data are shown in Figures 5e and 5f. At both seasonal and long-term
286 average time scales, there is no clear relationship shown between P and E_p , confirming the
287 independence between P and E_p discussed in Section 2.1.3. This result shows the difference
288 between E_p and E_{pa} , that E_p is independent from P but E_{pa} is not. Therefore, it is important to
289 distinguish E_{pa} from E_p and to understand the different physical mechanisms of the two processes
290 (Brutsaert, 2015).



291



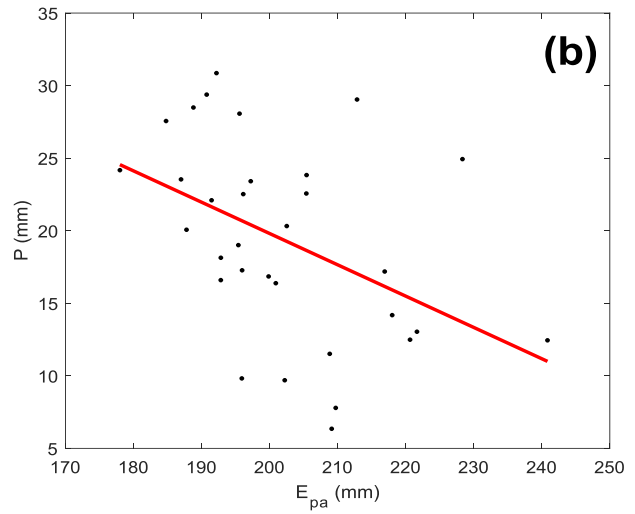
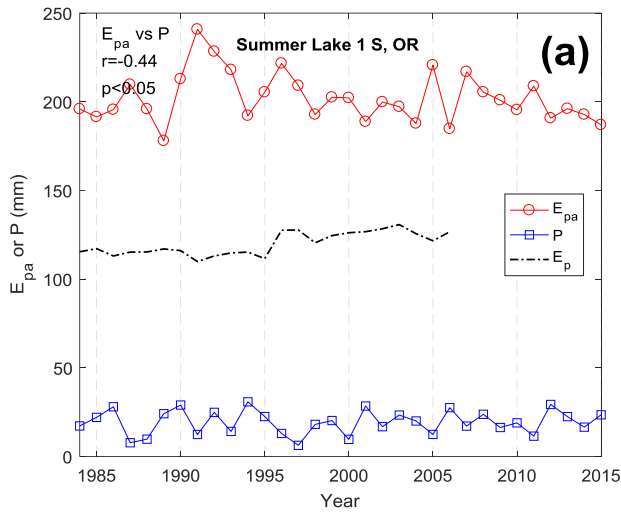
292



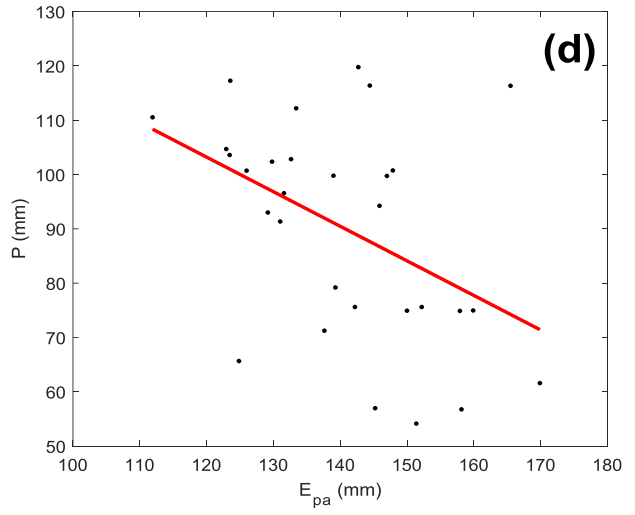
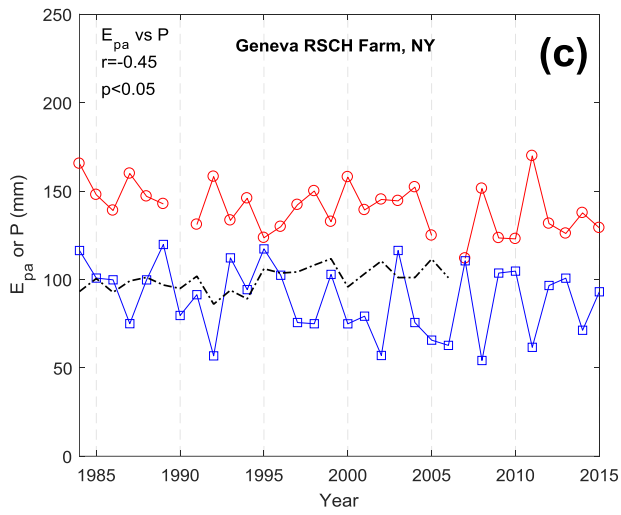
293

294 Fig. 5. P vs. E_{pa} at 259 weather stations in the US for the period 1984 to 2015 for (a) warm-
295 season data (N=5312), and (b) long-term annually averaged warm-season data (N=259). The
296 data points are color coded based on their latitudes and longitudes. P vs. E_{pa} at 93 weather
297 stations in the US for the period 1984 to 2001 using the homogenized pan evaporation dataset for
298 (c) warm period May-Oct in each year (N=1214), and (d) long-term annual average warm period
299 May-Oct data (N=93). P vs. E_p at the 259 weather stations for the period of 1984 to 2006 for (e)
300 warm-season data (N=5312) and (f) long-term annual average warm-season data (N=259).

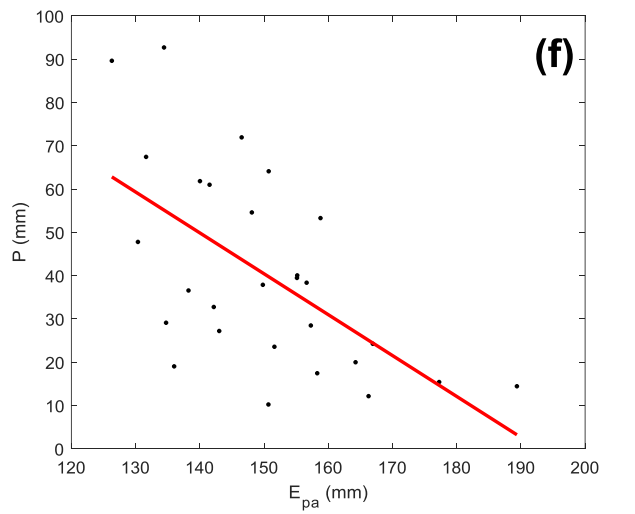
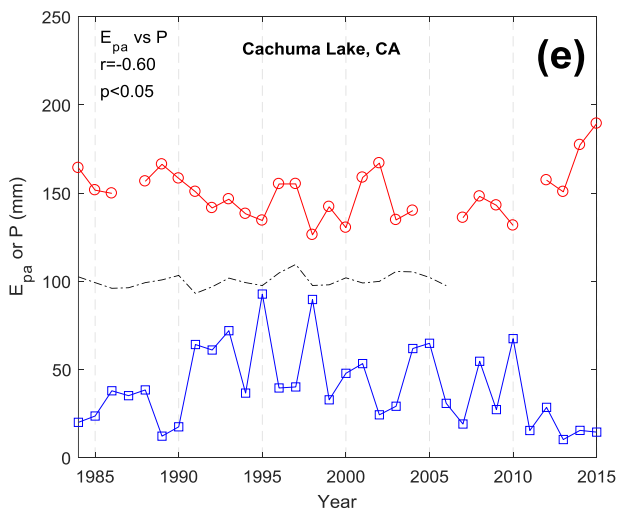
301 To present the P , E_p and E_{pa} relationships at individual locations and therefore to further
302 investigate the dependence between the three variables, we select four weather stations from the
303 four quadrants of the contiguous US (Fig. 3a), to show the warm-season P , E_p and E_{pa} in time
304 series (Fig. 6). The two stations in the southern regions have data in all 12 months of a year;
305 while the two stations in the northern regions only have E_{pa} data for six months of each year. All
306 four stations show negative correlations between P and E_{pa} . This negative correlation at the
307 weather station in Florida is not statistically significant (Figs. 6g and 6h). As mentioned before,
308 the P and E_{pa} correlation is less significant in the eastern region than in the west, because of the
309 wetter climate in the east. On the other hand, at the other three locations, the warm-season P and
310 E_{pa} are relatively symmetric to each other (Figs. 6a to 6f). During years when one series is above
311 average, the other tends to be below average and vice versa. In terms of the relationship between
312 P and E_p , all four locations show no significant correlations between the two variables ($p > 0.05$).
313 This is consistent with the independence of P and E_p shown in Fig. 5e and 5f.



314

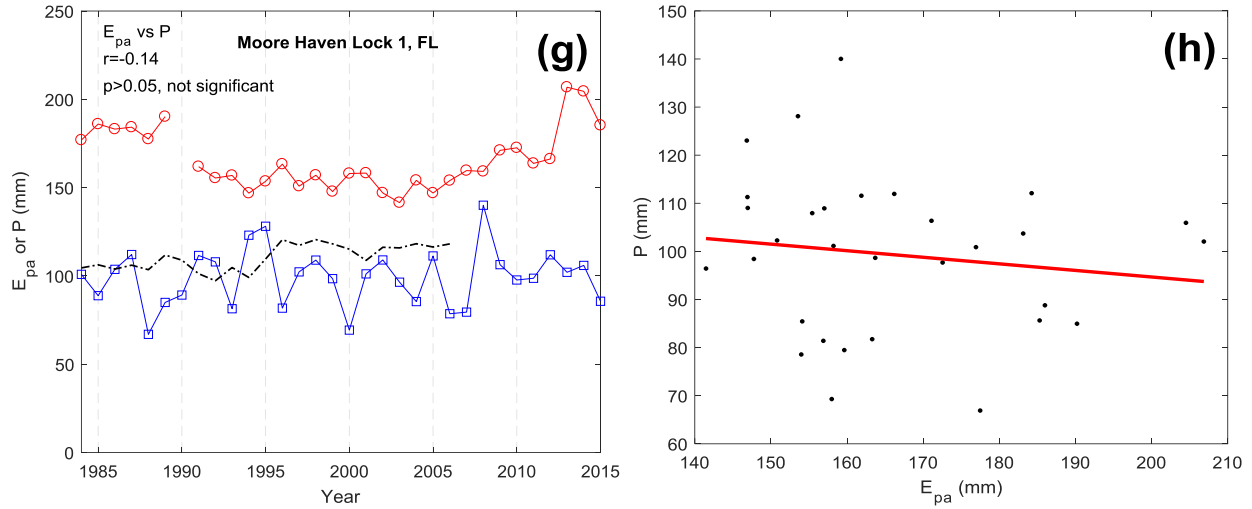


315



316

317



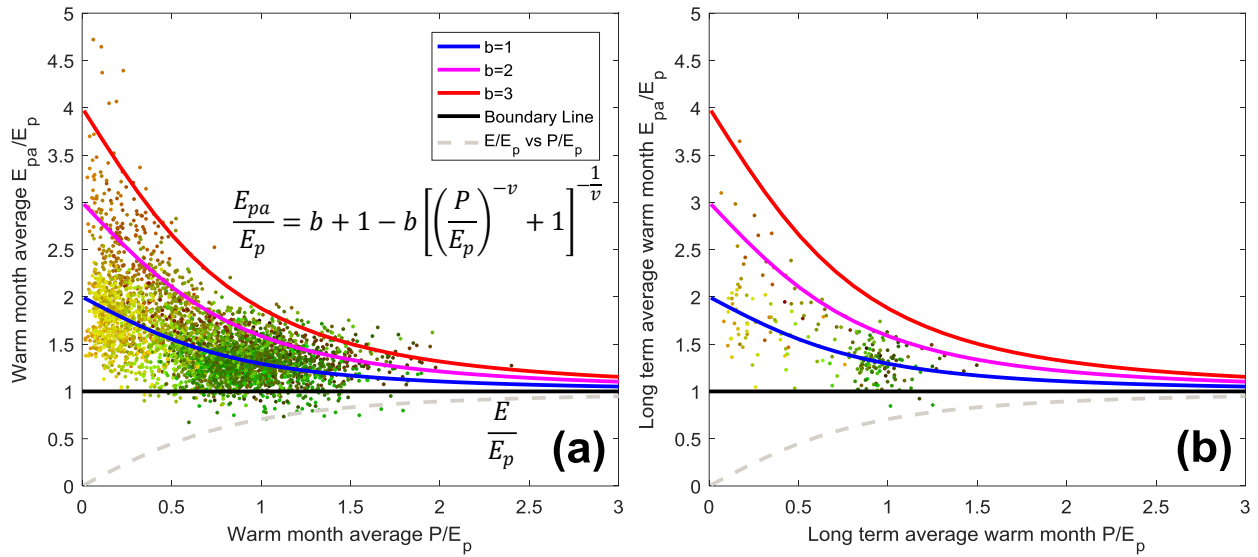
318

319 Fig. 6. Warm-season P , E_p and E_{pa} time series of four example weather stations in the study
 320 period of 1984-2015: (a) Summer Lake 1 S, OR (N 42°58', W 120°47'); (c) Geneva RSCH
 321 Farm, NY (N 42°53', W 77°20'); (e) Cachuma Lake, CA (N 34°35', W 119°59'); (g) Moore
 322 Haven Lock 1, FL (N 26°50', W 81°50'); and the scatterplots of P vs E_{pa} at the four example
 323 stations (b, d, f, h).

324 3.2 Bouchet-Budyko curves

325 There are two Bouchet-Budyko curves (Fig. 2). The upper curve describes the relationship
 326 between E_{pa} , E_p and P (Eq. 6) and the lower curve describes the relationship between E , E_p and P
 327 (Eq. 4). The lower curve is derived from the Budyko curve based on Turc-Pike equation. This
 328 relationship between E , E_p and P has been studied extensively following the Budyko framework
 329 and, therefore, it is not the focus of this study. This study investigates the relationship between
 330 E_{pa} , E_p and P , which is represented by the upper Bouchet-Budyko curve. Since the collected
 331 weather station data of P and E_{pa} are available 1984 to 2015 and the E_p data collected from the
 332 remote-sensing dataset are available 1983 to 2006, we examine the relationship between P/E_p
 333 and E_{pa}/E_p in the overlapping period of 1984 to 2006 (Fig. 7). Using Eq. (6) three curves with

334 different b values (1, 2, and 3) are shown in Figure 7. The ν value is set at 2, which is commonly
 335 used in the Budyko framework. When b equals one, the two CR curves are symmetric. When b
 336 exceeds one, the two CR curves are asymmetric. This asymmetry is discussed in previous
 337 studies (Kahler and Brutsaert, 2006; Brutsaert, 2015). One explanation of this asymmetry
 338 between E and E_{pa} is that the evaporation pan will receive more heat than the surrounding area
 339 (Kahler and Brutsaert, 2006). Brutsaert (2015) reports an even higher b values of 4.5. The
 340 horizontal solid black line in Fig. 7 is the boundary of the upper Bouchet-Budyko curve, above
 341 which E_{pa} exceeds E_p .



342
 343 Fig. 7. P/E_p vs. E_{pa}/E_p at 259 weather stations in the US for the period 1984 to 2015 for (a)
 344 warm-season data (N=5312), and (b) long-term average data (N=259). The data points are color
 345 coded based on their latitudes and longitudes. The three upper Bouchet-Budyko curves are
 346 plotted with different b values of $b=1$, $b=2$, and $b=3$, and with the same ν value of $\nu=2$. The
 347 dashed line is the lower Bouchet-Budyko curve with $\nu=2$.

348

349 4. Discussion

350 4.1 Relationship between P and E_{pa} , and between P and E_p

351 With the weather station data, a negative correlation between warm-season P and E_{pa} is shown in
352 242 out of 259 weather stations (93%). The negative correlation between P and E_{pa} is linked by
353 the humidity deficit. The formation of precipitation is positively related to the local level of
354 humidity (Pal et al., 2000; Sheffield et al., 2006; An et al., 2017) while “apparent” potential
355 evaporation is inversely related to humidity or positively related to the humidity deficit (Penman,
356 1948; Allen et al., 1998). As a result, precipitation and “apparent” potential evaporation will
357 tend to exhibit a negative correlation. According to the Bouchet’s complementary relationship,
358 this negative correlation between P and E_{pa} is more pronounced in arid regions than in humid
359 regions.

360 On the other hand, P and E_p shows no significant correlation at both the seasonal and the
361 long-term average time scales. As a result, our study indicates that potential evaporation and
362 precipitation, the representations of energy supply and water supply, are likely to be independent.
363 This independence is currently under investigation with field data. It should be noted that the
364 relationship between P and E_p and between P and E_{pa} found in this study are not direct causal
365 relationships, but rather the result of interactions between a number of physical variables, such as
366 net radiation, wind speed, humidity, and so forth. Further investigation into the physical
367 mechanisms connecting these variables is underway.

368 4.2 The Bouchet-Budyko curve and its applications

369 Combining the Bouchet’s complementary relationship and the Budyko framework leads to two
370 dimensionless CR curves, normalized by E_p (Fig. 2). The upper Bouchet-Budyko curve is
371 derived from the connection between Budyko framework and the CR, and the lower Bouchet-

372 Budyko curve is derived directly from the Budyko framework, based on the Turc-Pike equation.
373 The companion CR curves show that as the wetness index P/E_p decreases, the difference
374 between E and E_{pa} grows. This indicates the complementary relationship between E and E_{pa} is
375 most pronounced in arid environments; that is, the CR is more significant under water-limited
376 condition. As discussed in Ramírez et al. (2005), the CR can be considered as an extension of
377 the Budyko framework.

378 The P , E_p and E_{pa} collected in this study are following the general trend of the upper
379 Bouchet-Budyko curve (Fig. 7). The remote-sensing data of E_p may not have the same level of
380 accuracy as the field measured P and E_{pa} . The value of α in the Eq. (7) may vary from location
381 to location (Chen and Brutsaert, 1995; Brutsaert and Chen, 1995). Such factors may explain the
382 deviation of some data points from the CR curve in Fig. 7.

383 This upper Bouchet-Budyko curve can be used to estimate the E_{pa} based on the data of P
384 and E_p . The “apparent” potential evaporation can be measured by evaporation pan, but this
385 measurement has its limitations. For example, it is only available for warm periods. The
386 collected data with time averaged pan evaporation levels over weeks, months, and years may
387 lead to systematic error in surface flux calculations (Brutsaert, 1982; Kahler and Brutsaert,
388 2006). The Bouchet-Budyko curve can help us to estimate E_{pa} without the limitations of
389 evaporation pans. Comparing with more physically based E_{pa} quantification approaches, such as
390 Penman equation (Penman, 1948) and “PenPan” model (Rotstayn et al., 2006), our model is
391 derived from conceptual frameworks and therefore may provide top-down insights about the E_{pa}
392 level in hydrologic systems.

393 Similar to the Budyko framework, the Bouchet-Budyko curves can be used in hydrologic
394 models and climate models. These Bouchet-Budyko curves can be used to examine the fidelity

395 of simulated precipitation and evaporation sequences routinely produced by general circulation
396 models to drive climate change investigations.

397

398 **5. Conclusions**

399 We collected warm-season precipitation, potential evaporation, and “apparent” potential
400 evaporation data at 259 weather stations in the US to investigate the correlation among these
401 three physical variables. The results showed a negative correlation between P and E_{pa} at 93% of
402 the stations. The physical reason for the P , E_{pa} negative correlation could be related to the
403 humidity variability. When humidity increases, the likelihood for precipitation increases while
404 the rate of “apparent” potential evaporation decreases. On the other hand, our study results
405 supported the assumption that P and E_p are independent. Combining the CR with a Budyko-type
406 equation, we formulated the companion CR curves, showing the connection between the Bouchet
407 and Budyko frameworks. These insights may encourage hydrologists to further explore the
408 strong link between the Budyko framework and the CR, promoting new ways of hydrologic
409 modeling. Future work will investigate the physical mechanisms behind the newly-derived
410 Bouchet-Budyko curves and explore the application of these companion curves.

411

412 **Acknowledgment**

413 We thank the Editor and the three anonymous reviewers for their insightful and critical
414 comments and valuable suggestions. The data of precipitation and pan evaporation
415 measurements can be downloaded from the National Climatic Data Center website:
416 <https://www.ncdc.noaa.gov/IPS/cd/cd.html>. The homogenized pan evaporation data can be

417 downloaded from the USGS ScienceBase: <https://www.sciencebase.gov/catalog/>. The data of
418 remote-sensing based potential evaporation are provided by the Numerical Terradynamic
419 Simulation Group at University of Montana, based on the study of Zhang et al. (2010). The data
420 can be downloaded from their website: <http://www.ntsg.umt.edu/about/default.php>.

421

422 **References**

423 Allen, R. G., Pereira, L. S., Raes, D., and Smith, M. (Eds.): Crop evapotranspiration: Guidelines
424 for computing crop water requirements, Irrig. Drainage Pap. 56, Food and Agric. Org., Rome,
425 1998.

426 Aminzadeh, M., Roderick, M. L., and Or, D.: A generalized complementary relationship
427 between actual and potential evaporation defined by a reference surface temperature, *Water*
428 *Resour. Res.*, 52, 385-406, doi:10.1002/2015WR017969, 2015.

429 An, N., Wang, K., Zhou, C., and Pinker, R. T.: Observed variability of cloud frequency and
430 cloud-based height within 3600 m above the surface over the contiguous United States, *J.*
431 *Climate*, 30, 3725-3742, doi:10.1175/JCLI-D-16-0559.1, 2017.

432 Arora, V. K.: The use of the aridity index to assess climate change effect on annual runoff, *J.*
433 *Hydrol.*, 265, 164-177, 2002.

434 Bouchet, R.: Evapotranspiration réelle et potentielle, signification climatique, *IAHS Publ.*, 62,
435 134-142, 1963.

436 Brutsaert, W.: *Hydrology: An Introduction*, Cambridge Univ. Press, N. Y., 2005.

437 Brutsaert, W. and Chen, D.: Desorption and the two stages of drying of natural tallgrass prairie,
438 Water Resour. Res., 31, 1305-1313, 1995.

439 Brutsaert, W. and Parlange, M. B.: Hydrologic cycle explains the evaporation paradox, Nature,
440 396(5), 300, 1998.

441 Brutsaert, W. and Stricker, H.: An advection-aridity approach to estimate actual regional
442 evapotranspiration, Water Resour. Res., 15(2), 443-450, 1979.

443 Brutsaert, W.: A generalized complementary principle with physical constraints for land-surface
444 evaporation, Water Resour. Res., 51, 8087-8093, doi:10.1002/2015WR017720, 2015.

445 Brutsaert, W.: Evaporation into the Atmosphere: Theory, History and Applications, 299 pp.,
446 Springer, New York, 1982.

447 Budyko, M. I.: Climate and Life, translated from Russian by D. H. Miller, Elsevier, New York,
448 1974.

449 Budyko, M. I.: The Heat Balance of the Earth's Surface, U.S. Dep. of Commer., Washington, D.
450 C, 1958.

451 Carmona, A. M., Poveda, G., Sivapalan, M., Vallejo-Bernal, S. M., and Bustamante, E.: A
452 scaling approach to Budyko's framework and the complementary relationship of
453 evapotranspiration in humid environments: case study of the Amazon River basin, Hydrol. Earth
454 Syst. Sci., 20, 589-603, 2016.

455 Chen, D. and Brutsaert, W.: Diagnostics of land surface spatial variability and water vapor flux,
456 J. Geophys. Res., 100, 25,595-25,606, 1995.

457 Chen, X., Alimohammadi, N., and Wang, D.: Modeling interannual variability of seasonal
458 evaporation and storage change based on the extended Budyko framework, *Water Resour. Res.*,
459 49, 6067-6078, doi:10.1002/wrcr.20493, 2013.

460 Cheng, L., Xu, Z., Wang, D., and Cai, X.: Assessing inter-annual variability of ET at the
461 catchment scale using satellite-based ET datasets, *Water Resour. Res.*, 47, W09509,
462 doi:10.1029/2011WR010636, 2011.

463 Donohue, R. J., Roderick, M. L., and McVicar, T. R.: On the importance of including vegetation
464 dynamics in Budyko's hydrological model, *Hydrol. Earth Syst. Sci.*, 11, 983-995,
465 doi:10.5194/hess-11-983-2007, 2007.

466 Fu, B. P.: On the calculation of the evaporation from land surface [in Chinese], *Sci. Atmos. Sin.*,
467 5, 23-31, 1981.

468 Hobbins, M. T., Barsugli, J. J., Dewes, C. F., and Rangwala, I.: Monthly pan evaporation data
469 across the continental United States between 1950-2001, doi:10.21429/C9MW25, 2017.

470 Hobbins, M. T., Ramírez, J. A., and Brown, T. C.: Trends in pan evaporation and actual
471 evapotranspiration across the conterminous U.S.: Paradoxical or complementary?, *Geophys. Res.*
472 *Lett.*, 31, doi:10.1029/2004GL019846, 2004.

473 Jiang, L. and Islam, S.: Estimation of surface evaporation map over southern Great Plains using
474 remote sensing data, *Water Resour. Res.*, 37(2), 329-340, 2001.

475 Kahler, D. M., and Brutsaert, W.: Complementary relationship between daily evaporation in the
476 environment and pan evaporation, *Water Resour. Res.*, 42, W05413,
477 doi:10.1029/2005WR004541, 2006.

478 Lhomme, J. and Moussa, R.: Matching the Budyko functions with the complementary
479 evaporation relationship: consequences for the drying power of the air and the Priestley-Taylor
480 coefficient, *Hydrol. Earth Syst. Sci.*, 20, 4857-4865, doi:10.5194/hess-20-4857-2016, 2016.

481 Linacre, E. T.: Estimating U.S. class A pan evaporation from few climate data, *Water Int.*, 19(1),
482 5-14, 1994.

483 Milly, P. C. D.: Climate, soil water storage, and the average annual water balance, *Water Resour.*
484 *Res.*, 30, 2143-2156, 1994.

485 Morton, F. I.: Climatological estimates of evapotranspiration, *J. Hydraul. Div.*, 102(3), 275-291,
486 1976.

487 Pal, J. S., Small, E. E., and Eltahir, E. A. B.: Simulation of regional-scale water and energy
488 budgets: Representation of subgrid cloud and precipitation processes within RegCM, *J. Geophys.*
489 *Res.*, 105, 29,579-29,594, 2000.

490 Penman, H. L.: Natural evaporation from open water, bare and grass, *Proc. R. Soc., Ser. A*, 193,
491 120-145, 1948.

492 Pike, J. G.: The estimation of annual run-off from meteorological data in a tropical climate, *J.*
493 *Hydrol.*, 2(2), 116-123, 1964.

494 Potter, N. J., and Zhang, L.: Interannual variability of catchment water balance in Australia, *J.*
495 *Hydrol.*, 369, 120-129, 2009.

496 Priestley, C. H. B. and Taylor, R. J.: On the assessment of surface heat flux and evaporation
497 using large-scale parameters, *Mon. Weather Rev.*, 100(2), 81-92, 1972.

498 Ramírez, J. A., Hobbins, M. T., and Brown, T. C.: Observational evidence of the complementary
499 relationship in regional evaporation lends strong support for Bouchet's hypothesis, *Geophys.*
500 *Res. Lett.*, 32, L15401, doi:10.1029/2005GL023549, 2005.

501 Roderick, M. L., Hobbins, M. T., and Farquhar, G. D.: an evaporation trends and the terrestrial
502 water balance. II. Energy balance and interpretation, *Geogr. Compass*, 761-780,
503 doi:10.1111/j.1749-8198.2008.00214.x, 2009.

504 Rotstayn, N. D., Roderick, M. L., and Farquhar, G. D.: A simple pan-evaporation model for
505 analysis of climate simulations: Evaluation over Australia, *Geophys. Res. Lett.*, 33,
506 doi:10.1029/2006GL027114, 2006.

507 Sheffield, J., Goteti, G., and Wood, E. F.: Development of a 50-year high-resolution global
508 dataset of meteorological forcings for land surface modeling, *J. Climate*, 19, 3088-3111, 2006.

509 Shuttleworth, W. J.: Evaporation, in *Handbook of Hydrology*, edited by D. R. Maidment, pp.
510 4.1-4.53, McGraw-Hill, New York, 1993.

511 Stanhill, G.: The CIMO international evaporimeter comparisons, Publication 449, World
512 Meteorological organization, Geneva, 38 pp, 1976.

513 Thornthwaite, C. W.: An approach toward a rational classification of climate, *Geogr. Rev.*, 38,
514 55-94, 1948.

515 Turc, L.: Le bilan d'eau des sols: Relation entre les précipitations, l'évaporation et l'écoulement,
516 *Ann. Agron.*, 5, 491-569, 1954.

517 Van Bavel, C. H. M.: Potential evaporation: The combination concept and its experimental
518 verification, *Water Resour. Res.*, 2, 455-467, doi:10.1029/WR002i003p00455, 1966.

519 Wang, D. and Alimohammadi, N.: Responses of annual runoff, evaporation, and storage change
520 to climate variability at the watershed scale, *Water Resour. Res.*, 48, W05546,
521 doi:10.1029/2011WR011444, 2012.

522 Wang, D. and Tang, Y.: A one-parameter Budyko model for water balance captures emergent
523 behavior in Darwinian hydrologic models, *Geophys. Res. Lett.*, 41, 4569-4577,
524 doi:10.1002/2014GL060509, 2014.

525 Xu, X., Yang, D., Yang, H., and Lei, H.: Attribution analysis based on the Budyko hypothesis
526 for detecting the dominant cause of runoff decline in Haihe basin, *J. Hydrol.*, 510, 530-540,
527 doi:10.1016/j.jhydrol.2013.12.052, 2014.

528 Yang, D., Sun, F., Liu, Z., Cong, Z., and Lei, Z.: Interpreting the complementary relationship in
529 non-humid environments based on the Budyko and Penman hypotheses, *Geophys. Res. Lett.*, 33,
530 L18402, doi:10.1029/2006GL027657, 2006.

531 Yang, D., Sun, F., Liu, Z., Cong, Z., Ni, G., and Lei, Z.: Analyzing spatial and temporal
532 variability of annual water-energy balance in nonhumid regions of China using the Budyko
533 hypothesis, *Water Resour. Res.*, 43, 1-12, doi:10.1029/2006WR005224, 2007.

534 Yang, H. and Yang, D.: Derivation of climate elasticity of runoff to assess the effects of climate
535 change on annual runoff, *Water Resour. Res.*, 47, doi:10.1029/2010WR009287, 2011.

536 Yang, H., Yang, D., Lei, Z., and Sun, F.: New analytical derivation of the mean annual water-
537 energy balance equation, *Water Resour. Res.*, 44, W03410, doi:10.1029/2007WR006135, 2008.

538 Zhang, K., Kimball, J. S., Nemani, R. R., and Running, S. W.: A continuous satellite-derived
539 global record of land surface evapotranspiration from 1983 to 2006, *Water Resour. Res.*, 46,
540 W09522, doi:10.1029/2009WR008800, 2010.

541 Zhang, L., Dawes, W. R., and Walker, G. R.: Response of mean annual evapotranspiration to
542 vegetation changes at catchment scale, *Water Resour. Res.*, 37, 701-708, 2001.

543 Zhang, L., Potter, N., Hickel, K., Zhang, Y., and Shao, Q.: Water balance modeling over variable
544 time scales based on the Budyko framework – Model development and testing, *J. Hydrol.*, 360,
545 117-131.

546 Zhou, S., Yu, B., Huang, Y., and Wang, G.: The complementary relationship and generation of
547 the Budyko functions, *Geophys. Res. Lett.*, 42, 1781-1790, doi:10.1002/2015GL063511, 2015.

548 Zhou, S., Yu, B., Zhang, L., Huang, Y., Pan, M., and Wang, G.: A new method to partition
549 climate and catchment effect on the mean annual runoff based on the Budyko complementary
550 relationship, *Water Resour. Res.*, 52, doi:10.1002/2016WR019046, 2016.